Dispersion of Marked Fluid Elements in a Turbulent Ekman Layer

LARS-ARNE RAHM AND URBAN SVENSSON

The Swedish Meteorological and Hydrological Institute, S-601 76 Norrköping, Sweden

(Manuscript received 26 February 1986, in final form 24 June 1986)

ABSTRACT

A stochastic model is derived for studying shear-dispersion in a horizontally homogeneous, turbulent Ekman layer that is evolving in time. It is based on a one-dimensional model including an advanced turbulence closure ($k - \epsilon$) model, which yields the turbulent Ekman layer flow. A modified Langevin's equation is used to derive a Markov equation for the cross-flow velocity fluctuations in this inhomogeneous flow. Necessary statistical data for the Markov process are obtained from the $k - \epsilon$ model. Trajectories of marked fluid elements are then determined. Statistical properties of the dispersion process are calculated from the evolution of the cluster of marked fluid elements. The model is first applied to a plane Poiseuille flow. The results of the dispersion process are in good agreement with other, independent, estimates of dispersion in such a flow. A wind-driven Ekman layer is then considered. The results obtained agree well with data from tracer experiments in the ocean.

1. Introduction

Dispersion in a time-dependent, horizontally homogeneous turbulent Ekman layer is of interest both for practical and scientific reasons. In the present work the dispersion of marked fluid elements without inertia in a turbulent Ekman layer is calculated by a simulation of individual particle trajectories. The model to be described is based on the assumption that the dispersion process may be approximately described by a combination of vertical shear of a horizontal current and vertical diffusion. The theory of shear-flow dispersion began with Taylor's (1953) realization that the velocity shear in a pipe or channel would interact with cross-channel diffusion to produce an augmented along-channel dispersion. A thorough review of this process may be found in Csanady (1973).

The horizontal velocity field of the turbulent Ekman layer is obtained by the use of a one-dimensional boundary-layer model including a turbulence closure ($k - \epsilon$) scheme. The $k - \epsilon$ model seems to be a good compromise between complexity and generality, while keeping within the eddy-viscosity concept. However, it is based on a number of simplifying assumptions (one length scale, one time scale, high Reynolds numbers, the Prandtl/Kolmogrov relation, etc.) and also utilizes experimentally found relations (decay of grid turbulence, local equilibrium in near-wall regions, etc.). It is thus not suited for studies of turbulence, but has been found (see Rodi, 1980) to predict realistic eddy-viscosity profiles in a number of shear-flows. Details of the $k - \epsilon$ model as applied to the Ekman layer can be found in Svensson (1979).

The vertical diffusion is represented by a single-particle Markov process, analogous to what was proposed in the seminal paper by Obukhov (1959). Hence the vertical velocities of the particles obey an equation of motion of the Langevin's equation type, which is constituted by a random acceleration and a linear drag.

This approach has been used in a geophysical context in connection with some boundary-layer meteorology problems with good results (e.g., see Smith, 1968; Hall, 1975; Reid, 1979). It becomes less accurate, however, when applied to cases with vertically inhomogeneous turbulence. It will, for example, predict a too large and unrealistic drift of particles toward the ground in a case dealing with the planetary boundary layer (Wilson et al., 1981).

In order to eliminate this deficiency Wilson et al. (1981) have developed a method in which the original inhomogeneous turbulence field is transformed to a homogeneous one in order to circumvent this problem. Legg and Raupach (1982) presented an alternative approach, where the pressure gradient caused by the spatial variation in cross-stream velocity variance, i.e., the Reynolds stress, is incorporated into Langevin's equation. (It has been shown by Wilson et al., 1983, that both models give similar results in many cases, but that the new one presented in the same work is superior in inhomogeneous turbulence.) However, Thomson (1984) has made a rigorous derivation of the Markov chain model, and he showed both the benefits and weaknesses of the various models. The approach by Legg and Raupach (1982) is, however, going to be used in the present work. Though it is lacking generality, it is applicable for weakly inhomogeneous cases. The novel feature with this work is that one obtains the necessary statistical information "continuously" from the turbulence closure model mentioned above. This will facilitate the application of the dispersion model

to more complex time-dependent cases, such as—in this work—transient Ekman layers.

In order to test the complete model, it is first applied to a plane Poiseuille flow. The predicted velocity profile and the dispersion coefficients obtained agree well with laboratory and theoretical estimates, respectively, hence encouraging further work with dispersion in turbulent Ekman layers. The results obtained from the latter, rather idealized, case (horizontally homogeneous flow, stationary wind-stress and nonstratified conditions) are, however, in good agreement with tracer data from the oceanic surface layer (Okubo, 1971; Lam et al., 1984). This corroborates our proposition that horizontal dispersion in the Ekman layer is only, to lowest order and for moderate time and length scales, the result of vertical shear and vertical diffusion. The turbulent fluctuations in the horizontal plane are, as mentioned previously, neglected. One consequence of this result is a drastic simplification in the parameterization of the horizontal mixing processes in Ekman surface layers. (Note that the proposed process is in some ways analogous to the dispersion process in an oscillatory, sheared-velocity field of an internal wave, which has been discussed by Young et al., 1982, and Mollo-Christensen and Worthem, 1985.)

The outline of the paper is as follows. The vertical dispersion model and its background are discussed in section 2. The $k-\epsilon$ model is presented in section 3 together with its application to a plane Poiseuille flow, while section 4 is devoted to the results of the dispersion process in an Ekman layer. Finally, summary and discussions are presented in section 5.

2. Langevin's equation

The present study is limited to a one-dimensional, horizontally homogeneous turbulent process. Since the typical time scales of the horizontal velocity field are long compared to those of the turbulent process, the statistical properties of the latter are assumed stationary. Assume also that these properties resemble a Gaussian process with an exponential Lagrangian autocorrelation function (equal to what was used in Taylor, 1921, who examined the case of one-dimensional dispersion in homogeneous turbulence.) The associated Lagrangian integral time scale is a measure of how long the motion of a particle is correlated to its past. Pasquill (1974) has, however, shown that, by comparing dispersion for different spectral shapes, the specification of the exact shape is not as important as a reasonable estimate of the associated time scale. The vertical fluctuations are described by a stochastic process.

Arnold (1974) has shown that Langevin's equation yields vertical velocities with the requested properties. Hence, it seems justifiable to use this equation in describing the particle velocities in a turbulent flow. It describes the motion of a fluid particle subject to both a random acceleration and a retarding force. (Note that Langevin's equation has its roots in two "worlds," the macroscopic "world" represented by the drag force, and the microscopic "world" connected to the fluctuating random force.) The two forces may be interpreted as components of the total force acting over different time scales on a particle of intermediate length scale. It has been applied with good results to such diverse topics as Brownian motion (Uhlenbeck and Ornstein, 1930) and dynamics of star clusters (Chandrasekhar, 1943). [In fact, the model proposed by Taylor (1921) for the random velocity of a single particle in homogeneous turbulence becomes, in the limit of small time scales, equivalent with Langevin's equation (Wax, 1954).]

Langevin's equation is defined in its most basic form (cf. Legg and Raupach, 1982, the analysis of which is briefly outlined below) as

$$\frac{dw}{dt} = \lambda\xi - \alpha w \tag{2.1}$$

where the vertical velocity of a particle is denoted $w(t)$. Here $\xi(t)$ represents a statistically stationary stochastic process. It is characterized by Gaussian white noise, a Gaussian probability density function, a mean of zero and a standard deviation, the latter of which is uncorrelated to w. The coefficients α and λ are going to be derived below. (Note, however, that the full Navier–Stokes equations of motion in Lagrangian form are characterized by nonlinear dissipative terms, while Langevin's equation has a linear one. This feature has been discussed by Krasnoff and Peskin, 1971, but an incorporation of, e.g., a quadratic dependence, is beyond the scope of this work.)

Equation (2.1) is solvable by conventional methods (e.g., see Arnold, 1974) despite its stochastic character. The solution becomes

$$w(t) = w(0)e^{-\alpha t} + \lambda \int_0^t \{e^{\alpha(s-t)}\xi(s)\}ds \tag{2.2}$$

where $w(0)$ is a random initial value.

By assuming both stationarity of the stochastic process and that ξ is uncorrelated to the vertical velocity, the covariance becomes

$$\sigma_w^2 = \overline{w'(t)^2} = \overline{w'(0)^2}e^{-2\alpha t} + \frac{\lambda^2}{2\alpha}\{1 - e^{-2\alpha t}\} \tag{2.3}$$

and hence

$$\sigma_w^2 = \frac{\lambda^2}{2\alpha}. \tag{2.4}$$

Here the velocity is supposed resolved into

$$w = \bar{w} + w' \tag{2.5}$$

where $\bar{w}$ and w' are the ensemble-average and its departure, respectively.

By definition, the Lagrangian integral time scale (sometimes in literature called the "correlation time") yields

$$\tau_l = \frac{1}{\overline{w'(0)^2}} \int_0^\infty \overline{w'(0)w'(t)}dt = \int_0^\infty e^{-\alpha t}dt = \frac{1}{\alpha}. \quad (2.6)$$

If the Lagrangian velocity statistics σ_w and τ_l are given, Eq. (2.1) will predict the vertical velocities of an ensemble of fluid particles with a prescribed initial velocity distribution. Since Langevin's equation is going to be used in the context of finite-difference equations, it is reformulated as a Markov sequence, defined at discrete times, $t_{n+1} - t_n = \Delta t$. The time step Δt must satisfy the unequality

$$\tau_\lambda \ll \Delta t \ll \tau_l \quad (2.7)$$

where τ_λ is of the order of the Taylor microscale of the Lagrangian autocorrelation time scale for acceleration of particles. This limitation is imposed in order to ensure that the particle velocity w_{n+1} only will depend on w_n and not on earlier events. Hence τ_λ has to be large enough to smooth out molecular irregularities in w (e.g., see Obukhov, 1959), as w represents a macroscopic velocity.

The Markov chain becomes

$$w_{n+1} = a_n w_n + b_n \sigma_{wn} \xi_n \quad (2.8)$$

where ξ_n is a random number from a Gaussian distribution with zero mean and unit variance. [Note that a slowly varying turbulence field is allowed in (2.8)]. A comparison of (2.8) with solution (2.2) yields

$$a_n = \bar{e}^{\Delta t/\tau_{ln}} \quad (2.9)$$

while a similar comparison between the variance of (2.8) and (2.3) results in

$$b_n = (1 - \bar{e}^{2\Delta t/\tau_{ln}})^{1/2}. \quad (2.10)$$

Equations (2.8)–(2.10) represent the model that was successfully used by Legg (1982), who compared predicted vertical dispersion from a line source in a horizontal wind with results from an analogous wind-tunnel experiment.

Hitherto the turbulent flow is assumed to be vertically homogeneous, such that both τ_l and σ_w are independent of position. If, however, a gradient in velocity variance exists (as it usually does close to boundaries), the present model becomes inadequate. Legg and Raupach (1982) showed how to incorporate the mean pressure gradient associated with the gradient in velocity variance in an incompressible turbulent flow (e.g., see Hinze, 1975). (For a detailed discussion on the limitations of this approach, see Thompson, 1984.) The pressure gradient becomes

$$F = \overline{\frac{\partial w_E'^2}{\partial z}} = -\frac{1}{\rho}\frac{\partial \bar{P}}{\partial z}. \quad (2.11)$$

(Hereafter, subscript E denotes the Eulerian variables.)

The Langevin's equation then becomes

$$\frac{dw}{dt} = \lambda \xi(t) - \alpha w + F. \quad (2.12)$$

Its solution, analogous to (2.2), turns out as

$$w(t) = w(0)e^{-\alpha t} + \lambda \int_0^t \{e^{\alpha(s-t)}\xi(s)\}ds + \frac{F}{\alpha}(1 - e^{-\alpha t}). \quad (2.13)$$

The variance and covariance functions still remain valid despite $F \neq 0$. However, the ensemble-average now exhibits a mean drift velocity due to the pressure gradient:

$$\bar{w} = \frac{F}{\alpha}. \quad (2.14)$$

The reformulated Markov chain becomes

$$w_{n+1} = a_n w_n + b_n \sigma_{wn} \xi_n + C_n \quad (2.15)$$

where consequently a_n and b_n remain unaltered, while a comparison of (2.13) with (2.15) yields

$$C_n = \frac{F}{\alpha}(1 - \bar{e}^{\Delta t/\tau_{ln}}). \quad (2.16)$$

Equation (2.15) is formulated in a Lagrangian frame of reference, but F is based on Eulerian properties. Hanna (1982) has, however, shown that the Eulerian variance is reasonably well approximated by its Lagrangian counterpart, thus assume

$$F = \frac{\partial}{\partial z}(\sigma_w^2). \quad (2.17)$$

Equation (2.15) is readily solved, if τ_{ln} and σ_{wn} are specified for each particle. (Note that an "external" velocity may be superimposed, representing, e.g., a sedimentation velocity, Ekman pumping, etc. The conditions for this superposition have, however, not been considered in this work.)

In addition to the initial values, boundary conditions have to be included in a finite-depth case. This is done by requiring that all particles, which reach a boundary, will be reflected. Hence zero flux conditions are applied.

3. Poiseuille flow

With the purpose of testing the predictions of the model, dispersion in a fully developed channel flow, a Poiseuille flow, is considered. The flow is determined by the previously mentioned turbulence closure model by Svensson (1979).

The steady-state momentum equation becomes

$$0 = -\frac{1}{\rho}\frac{\partial P}{\partial x} + \frac{\partial}{\partial z}\left(\frac{\mu_T}{\rho}\frac{\partial U}{\partial z}\right) \quad (3.1)$$

where U, P and ρ represent the horizontal velocity, the pressure and the density. The pressure gradient is calculated from (see Svensson, 1979)

$$\frac{\partial}{\partial t}\left(\frac{\partial P}{\partial x}\right) = C_p(\bar{U} - \bar{U}_p). \quad (3.2)$$

Here $\bar{U}$ and $\bar{U}_p$ are the mean velocity and the prescribed mean velocity, while C_p is a numerical coefficient.

Equation (3.2) yields a steady-state pressure gradient, where $\bar{U} = \bar{U}_p$, independently of C_p. The turbulent exchange coefficient μ_T is determined by the $k - \epsilon$ equations. The kinetic energy equation becomes

$$\frac{\partial k}{\partial t} = \frac{\partial}{\partial z}\left\{\frac{\mu_T}{\rho\sigma_k}\frac{\partial k}{\partial z}\right\} + \frac{\mu_T}{\rho}\left(\frac{\partial U}{\partial z}\right)^2 - \epsilon \tag{3.3}$$

while the dissipation equation is

$$\frac{\partial \epsilon}{\partial t} = \frac{\partial}{\partial z}\left\{\frac{\mu_T}{\rho\sigma_\epsilon}\frac{\partial \epsilon}{\partial z}\right\} + C_{1\epsilon}\frac{\mu_T}{\rho}\frac{\epsilon}{k}\left(\frac{\partial U}{\partial z}\right)^2 - C_{2\epsilon}\frac{\epsilon^2}{k} \tag{3.4}$$

$$\frac{\mu_T}{\rho} = C_\mu\frac{k^2}{\epsilon}. \tag{3.5}$$

The turbulent Prandtl/Schmidt numbers σ_k and σ_ϵ, as well as the empirical coefficients $C_{1\epsilon}$ and $C_{2\epsilon}$, are given in Table 1.

This set of equations is solved numerically in its finite-difference form by an implicit scheme and a standard tridiagonal matrix algorithm (Svensson, 1979). These equations and their solutions have been discussed extensively in the past. Hence the reader is referred to Svensson (1978) for further details. The present boundary conditions are represented by no-slip conditions at the rigid bottom, while, due to the symmetry of the problem, the boundary condition at the centerline is given by a zero shear. Boundary conditions for k and ϵ at the bottom are given by prescribed values related to the calculated shear stress. Due to the symmetry plane, zero flux conditions are prescribed at the upper boundary. (For details, see Svensson, 1978, or Rodi, 1980.) Though there are no straightforward relations between Lagrangian and Eulerian statistics (e.g., see Pasquill and Smith, 1983), the sought variables σ_w and τ_l may be approximately determined by the $k - \epsilon$ model. The latter defines typical turbulent velocity and time scales in an Eulerian frame of reference:

$$\tau_E = C_\tau k\epsilon^{-1} \tag{3.6}$$

$$\sigma_{wE}^2 = C_\sigma k \tag{3.7}$$

where C_τ and C_σ are empirically determined coefficients.

Estimates from experiments valid for near-wall turbulence by Launder et al. (1975) and Zeman and Tennekes (1975) yield $C_\sigma = 0.25$ and 0.34, respectively. Hence a reasonable choice may be 0.3. The Lagrangian variance then becomes, according to the previously mentioned assumption by Hanna (1982),

$$\sigma_w^2 = \sigma_{wE}^2 = C_\sigma k. \tag{3.8}$$

Pasquill (1974) has presented $C_\tau = 0.3$, while an estimate (Rodi, 1980) based on a Prandtl-length formulation yields $C_\tau = 0.16$. Hence an approximate value of 0.2 is chosen. Batchelor (1949) has shown that an effective exchange coefficient, based on Lagrangian properties, may be formulated as

$$\nu_T = \sigma_w^2\tau_l. \tag{3.9}$$

Assuming that this is equivalent with (3.5), one obtains

$$\tau_L = \frac{C_\mu k}{C_\sigma\epsilon}. \tag{3.10}$$

The ratio between the Lagrangian and Eulerian time scales then turns out as

$$\frac{\tau_l}{\tau_E} = \frac{C_\mu}{C_\sigma C_\tau}. \tag{3.11}$$

To summarize the above, σ_w and τ_l are calculated for each time and length step by the $k - \epsilon$ model. This information is then utilized in solving Langevin's equation. Since the time steps in the latter process may be quite small [within the restrictions (2.7)] compared to those in the $k - \epsilon$ model, the values of σ_w and τ_l are assumed constant for each time step and depth in the $k - \epsilon$ model.

In accordance with the experimental setup of Hussain and Reynolds (1975), the total depth of the fluid was 6.35×10^{-2} m. An airflow with a mean velocity $\bar{U}_p = 10.0$ m s^{-1} was chosen. The coefficient C_p in the pressure calculations was set to 5 (but its value will only influence the convergence speed of the calculations).

After the velocity field had reached a steady state, the longitudinal dispersion was calculated by following 500 particles, released from a line-source. They were advected with the current in the longitudinal direction and transported by turbulence in the cross-flow direction. The variance of the longitudinal spread was then calculated. An example of the evolution in time for the cluster of particles is shown in Fig. 1 for a case with two rigid boundaries. Since the integral time scale has a maximum at the level of symmetry plane and, further, σ_w has a minimum at the same level, one should expect an accumulation of particles in this region. However, due to the included effect of pressure gradients there is no tendency to accumulate near the symmetry plane. The trajectories of three randomly chosen particles are shown in Fig. 2. The decrease in integral time scale close to the boundaries is clearly noticeable.

An "apparent" eddy diffusivity may be defined according to Csanady (1973) (though originally presented

TABLE 1. Constants used in the calculations. The asterisks denote coefficients that occasionally have been altered in the purpose of testing the sensitivity of the model.

σ_k	σ_ϵ	$C_{1\epsilon}$	$C_{2\epsilon}$	C_μ	C_σ^*	C_τ^*
1.4	1.3	1.44	1.9	0.09	0.3	0.2

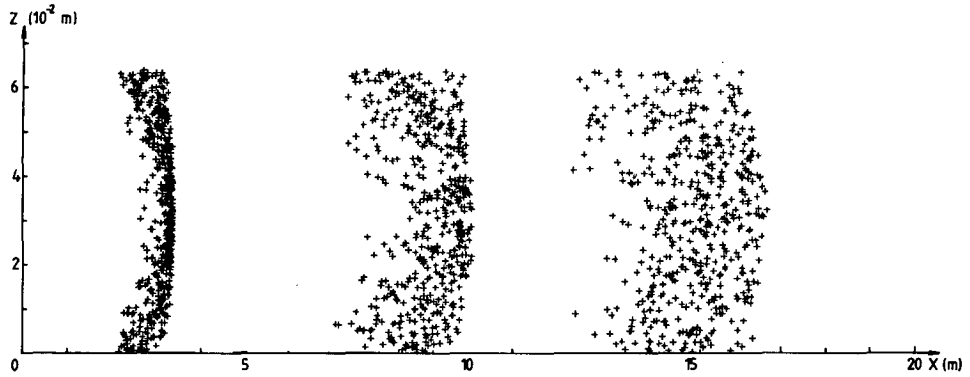

FIG. 1. Evolution of a cluster of particles is shown every 0.6 s.

by Batchelor, 1949, in a slightly more general form), as

$$E_d = \frac{1}{2}\frac{\partial}{\partial t}(\sigma_x^2) \tag{3.12}$$

where σ_x is the standard deviation of position in longitudinal direction. Since, to the best knowledge of the authors, there are no empirical data from exactly this case, comparisons have to be done with some similar cases.

Taylor (1954) has presented a relation for dispersion in a pipe:

$$E_d = 10.1 \times U_* \cdot r \tag{3.13}$$

where U_* and r represent the frictional velocity and the radius of the pipe, respectively. Elder (1959) gave a similar formula for a free-surface channel of depth d:

$$E_d = 5.9 \times U_* \cdot d. \tag{3.14}$$

When applied to the present case, Taylor's formula yields $E_d = 0.15$ m^2 s^{-1}, while the corresponding value based on (3.14) becomes $E_d = 0.18$ m^2 s^{-1}. Since the value obtained from our calculations, based on (3.12), is $E_d = 0.18$ m^2 s^{-1}, the agreement found seems quite good. Moreover, previous comparisons (Svensson, 1979) between the results from the $k - \epsilon$ model and the experimental data on channel flow reported by Hussain and Reynolds (1975) have revealed excellent agreement both for the velocity profiles and the eddy coefficients. Hence, as a conclusion, the present model seems to predict the essential properties of a plane Poiseuille flow with reasonable accuracy. Further, the simulated dispersion agrees well with previous estimates.

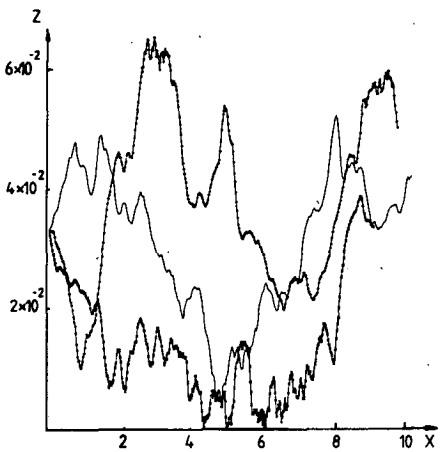

FIG. 2. Trajectories formed by three arbitrarily chosen particles during 1 sec after release.

4. Turbulent Ekman layer

The homogeneous turbulent Ekman surface layer is solved numerically by the same turbulence closure scheme as for the Poiseuille flow. The momentum equations become

$$\frac{\partial U}{\partial t} - fV = \frac{\partial}{\partial z}\left(\frac{\mu_T}{\rho}\frac{\partial U}{\partial z}\right) \tag{4.1a}$$

$$\frac{\partial V}{\partial t} + fU = \frac{\partial}{\partial z}\left(\frac{\mu_T}{\rho}\frac{\partial V}{\partial z}\right) \tag{4.1b}$$

where f represents the Coriolis parameter and U and V the horizontal velocities. As in the previous case, the exchange coefficient μ_T is determined for each time- and length-step by solutions to the $k - \epsilon$ equations. Only the quadratic terms in (3.3) and (3.4) are modified also to include $(\partial V/\partial z)^2$.

The present study is limited to a horizontally homogeneous, neutrally stratified flow in an unbounded area; consequently, no Ekman pumping takes place. Furthermore, the buildup of a pressure gradient and the associated geostrophic interior flow is excluded. This problem has also been investigated in the past by use of the $k - \epsilon$ model (Svensson, 1979). With the reservation that relevant experimental data from the surface layers are sparse, the predictions obtained seem to give a realistic description of the dynamics of the

transient, turbulent Ekman layer. The resulting dissipation rates, the velocity profile and the eddy viscosity distribution are all comparable with those given by Dillon and Powell (1976), Madsen (1977) and Shir (1973), respectively. (For further details, see Svensson, 1979.)

The ratio of the Lagrangian to Eulerian integral time scale becomes roughly [see (3.11)] 1.5. This is in reasonable agreement with independent estimates from the ocean and the atmosphere. Schott and Quadfasel (1979) reported a ratio of 1.4 ± 0.4 from measurements in the Baltic, while Hay and Pasquill (1959) have presented values around 4 from a wide range of experimental conditions. The uncertainties in the values chosen are, however, considerable. A simple test of the sensitivity of the complete model to variations in the coefficients chosen are reported later in this section.

The experimental setup was as follows. A cluster of 200 particles was released at a depth of 10 m in a horizontally unbounded, homogeneous layer of thickness 50 m. This occurred 6 hours after a steady wind had started blowing. The cloud spread was governed, as mentioned before, by the combined models of vertical turbulent mixing and turbulent Ekman-layer dynamics. (The evolution of the cluster with time is shown for one realization in Fig. 3.) Variance in horizontal projection of the particles was calculated for each time step of the $k - \epsilon$ model. The time step used in this model was 600 s, which yields a time-step independent solution. The choice of time step of the Markov process

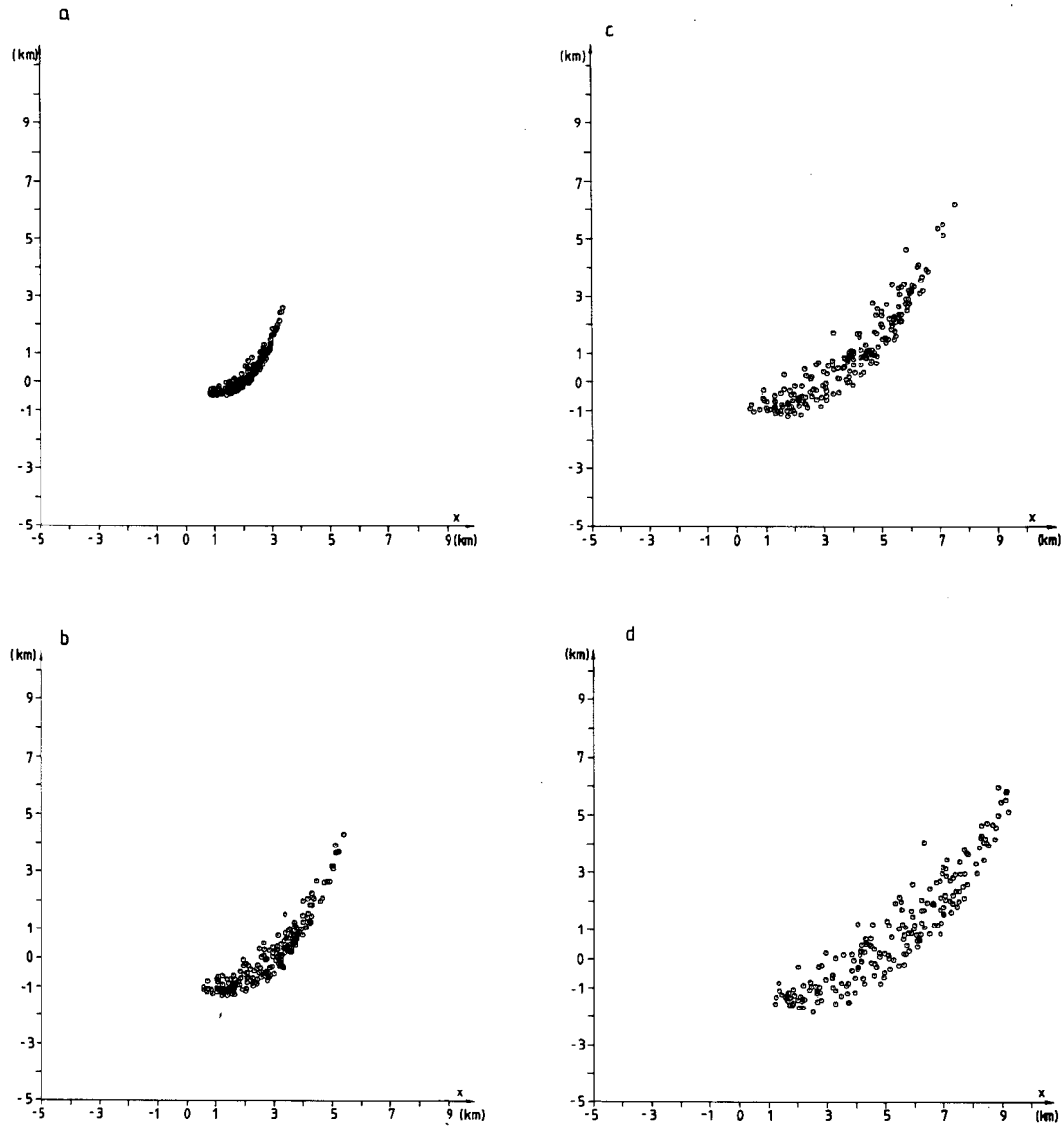

FIG. 3. Horizontal distribution of marked fluid elements: (a) 6 hours, (b) 12 hours, (c) 18 hours, and (d) 24 hours after release from "origin." A wind of strength 5 m s^{-1} is assumed blowing in the direction of the ordinate.

is governed by the inequality of (2.7). The Lagrangian time scale for a typical case becomes, according to Eq. (3.10), roughly 20 s in the surface layer but increases downward to approximately 2000 s close to the bottom. A typical distribution of τ_l for the present case is shown in Fig. 4.

The corresponding Taylor microscale, which according to Tennekes and Lumley (1972) may be expressed as

$$\tau_\lambda = \left(\frac{15\nu}{\epsilon}\right)^{1/2} \tag{4.2}$$

where ν represents the viscosity, falls within the range of 4 to 120 s. Hence, it is not possible to choose a Δt so that (2.7) is fulfilled everywhere. As a compromise, a time step of 50 s was chosen in order to ensure a reasonable region of validity. The errors induced by using a too large time step in a vicinity of the boundaries are assumed acceptable. Although this calculation was not carried out in the major and minor principal axis of the cluster but along the wind direction and transverse to it, the same approximation to a radially symmetric distribution, as given by Okubo (1971), was used:

$$\sigma_{rc}^2 = 2\sigma_x \cdot \sigma_y. \tag{4.3}$$

The evolution in time of this variance is presented in Fig. 5 in some cases with different forcing. (Note that each set of data is obtained from only one realization.) The data are sampled every 6 hours in the interval 12–132 hours (after the start of the wind forcing). For the case of intermediate forcing, even the evaluation of σ_{rc}^2 in the interval 6–18 hours is presented. The straight lines through each set of data are obtained by a linear regression analysis.

In order to study the sensitivity of the model, calculations with a 50% increase in C_τ were carried out, which resulted in an approximately 30% decrease in slope and magnitude of σ_{rc}^2. A 50% increase in C_σ was also carried out, resulting in an even slightly more pronounced decrease in slope and magnitude.

In order to compare the results with some tracer

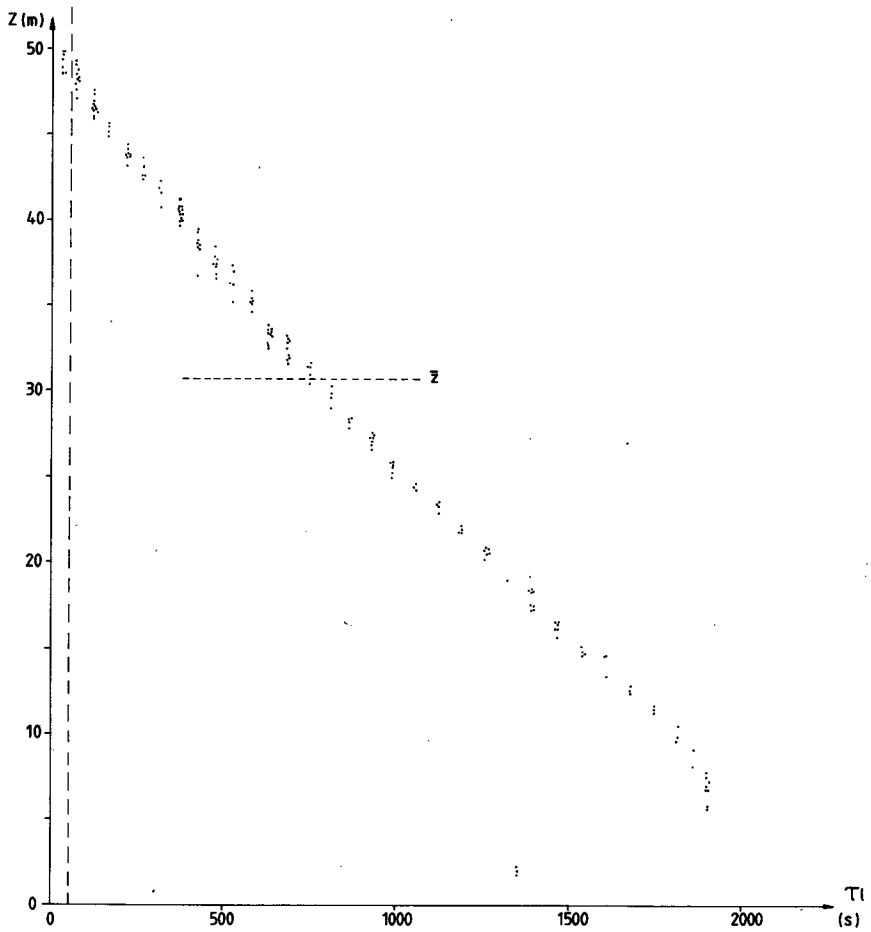

FIG. 4. Instantaneous distribution of marked fluid elements with height and their Lagrangian time scales respectively. The center of the cluster, $\bar{z}$, as well as the time steps (dotted) used in the Markov process are shown.

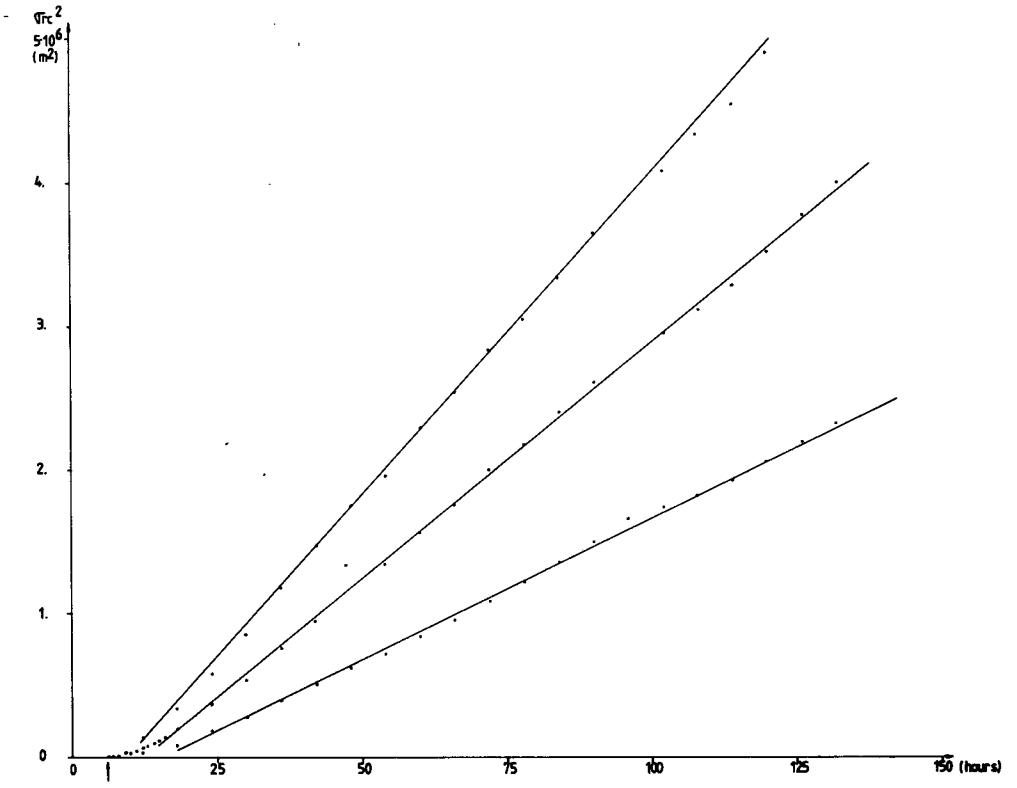

FIG. 5. The variance σ_{rc}^2 vs time for three different wind speeds: (a) 2 m s^{-1}, (b) 5 m s^{-1}, and (c) 8 m s^{-1}. The straight lines are obtained from a linear regression analysis.

data from field experiments in the oceans, the diffusion data summarized by Okubo (1971) and discussed by Csanady (1973) are presented (see Fig. 6) together with the present data. As a general conclusion, the latter collapse on the data obtained from field measurements. The effect of varying the degree of forcing is noticeable. However, the increase in σ_{rc}^2 with time is clearly slower than the corresponding variance based on Okubo's data. This is also confirmed by the logarithmic regression analysis presented in the same figure. The exponentials fall within the range 1.4–1.7, which should be compared with the mean value of 2.3, given by Okubo (1971), as is shown in Fig. 6. Analogous results but for $C_\sigma = 0.3$ and $C_\tau = 0.3$ are also presented (see Fig. 7).

Following Okubo (1971), an apparent diffusivity, K_a, may be defined as

$$K_a = \sigma_{rc}^2/4t. \tag{4.4}$$

The values fall within the range 1.4–3.1 m^2 s^{-1}, based on the same data as in Fig. 5. This order of magnitude agrees well with estimates presented in both Okubo (1971) and Lam et al. (1984).

An example of a momentaneous profile of the Lagrangian time scale is shown, as mentioned above, in Fig. 4, which is representative for the major part of the period. The effect of the turbulence-generating boundaries is readily seen. Though τ_l is proportional to k/ϵ, it is the dissipation that governs its distribution (though k varies in the same way but markedly slower). It varies roughly inversely with distance from the boundary. This feature, which is easily derived by a combination of the inertial subrange law and turbulent energy considerations (e.g., see Pasquill and Smith, 1983), has been observed in the planetary boundary layer by, for example, Zilitinkevitch et al. (1967). The Langevin's equation, in its finite-difference form (2.15), is derived within the assumption (2.7). This inequality is fulfilled everywhere except close to the boundaries, as is noticeable in the graph. This fact is assumed to be of minor importance in the calculations, something that has been confirmed by varying the time step. The distribution of velocity variance σ_w^2 is also shown (see Fig. 8).

The standard deviation of the width of the cluster in the direction of the wind and its evolution in time is presented in Fig. 9 for the same case as above. The gross behavior of the cloud spread is in accordance with what is expected from Ekman dynamics; the Ekman drift of the cluster as well as the inertial oscillations superimposed on the drift ($f = 10^{-4}$ s^{-1} yields a period of 17.5 h).

In the initial phase of cluster growth, the cluster will

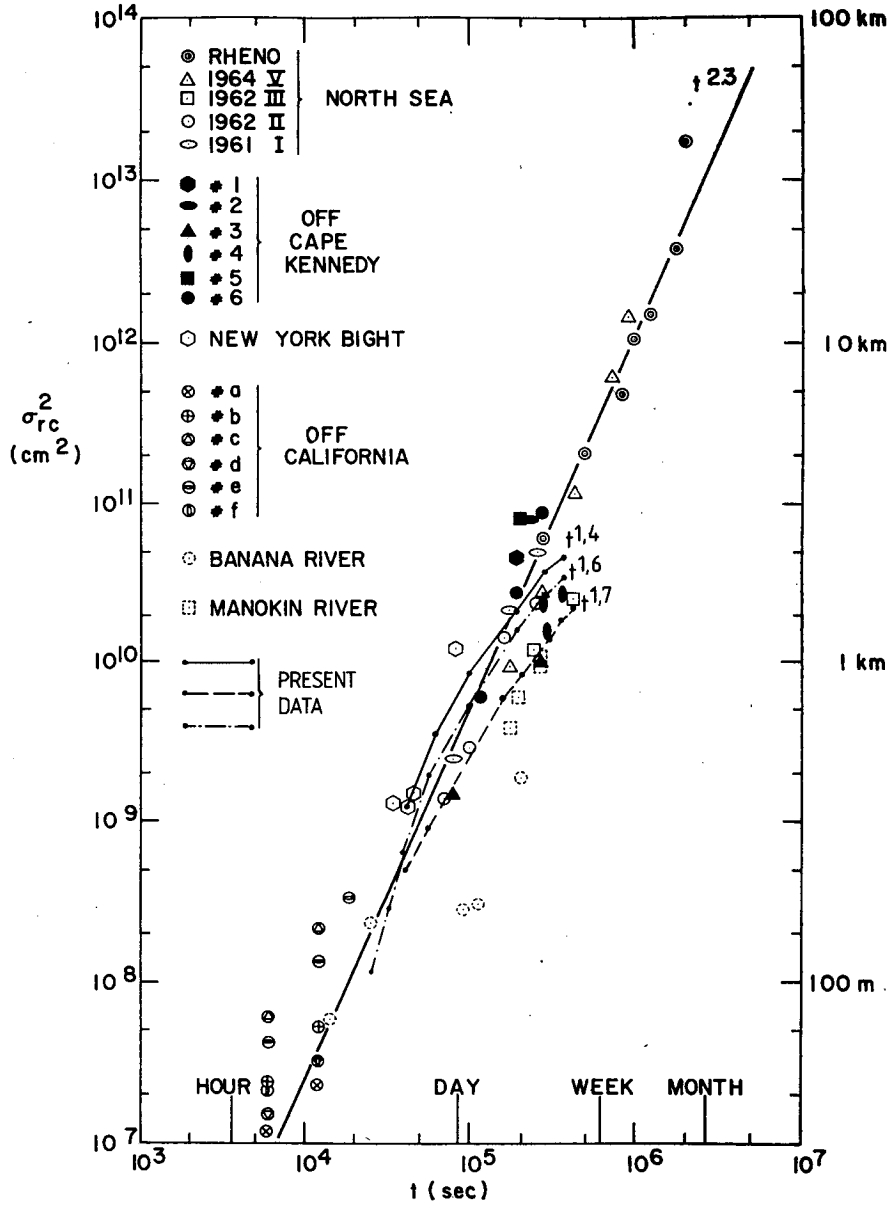

FIG. 6. A diffusion diagram for variance vs time from Okubo (1971). Data from three different wind speeds are shown: (a) 2 m s^{-1} (stippled), (b) 5 m s^{-1} (dashed), and (c) 8 m s^{-1} (solid). The growth rates are obtained by a logarithmic regression analysis in order to compare with the one by Okubo.

be transported by the Ekman flow simultaneously with a vertical spreading of the particles to depths of different flow and turbulence characteristics. This behavior is reflected in the evolution of the apparent horizontal diffusivity K_x, defined (cf. Csanady, 1973) as

$$K_x = \frac{1}{2}\frac{\partial}{\partial t}(\sigma_x^2). \tag{4.5}$$

These values are presented for the initial period (but only for one realization) in Fig. 10. The initially weak diffusivity increases rapidly with time and approaches asymptotically its stationary value. Hence the lateral and vertical extent of the domain of occupation increases rapidly in time until it approaches the characteristic size of the inertial oscillations. On time scales larger than the inertial period the evolution of the cluster becomes slower and almost linear (see also Fig. 5). The behavior observed here is in accordance with what is known of cluster growth (Csanady, 1973). It is, however, obtained without any horizontal diffusive process.

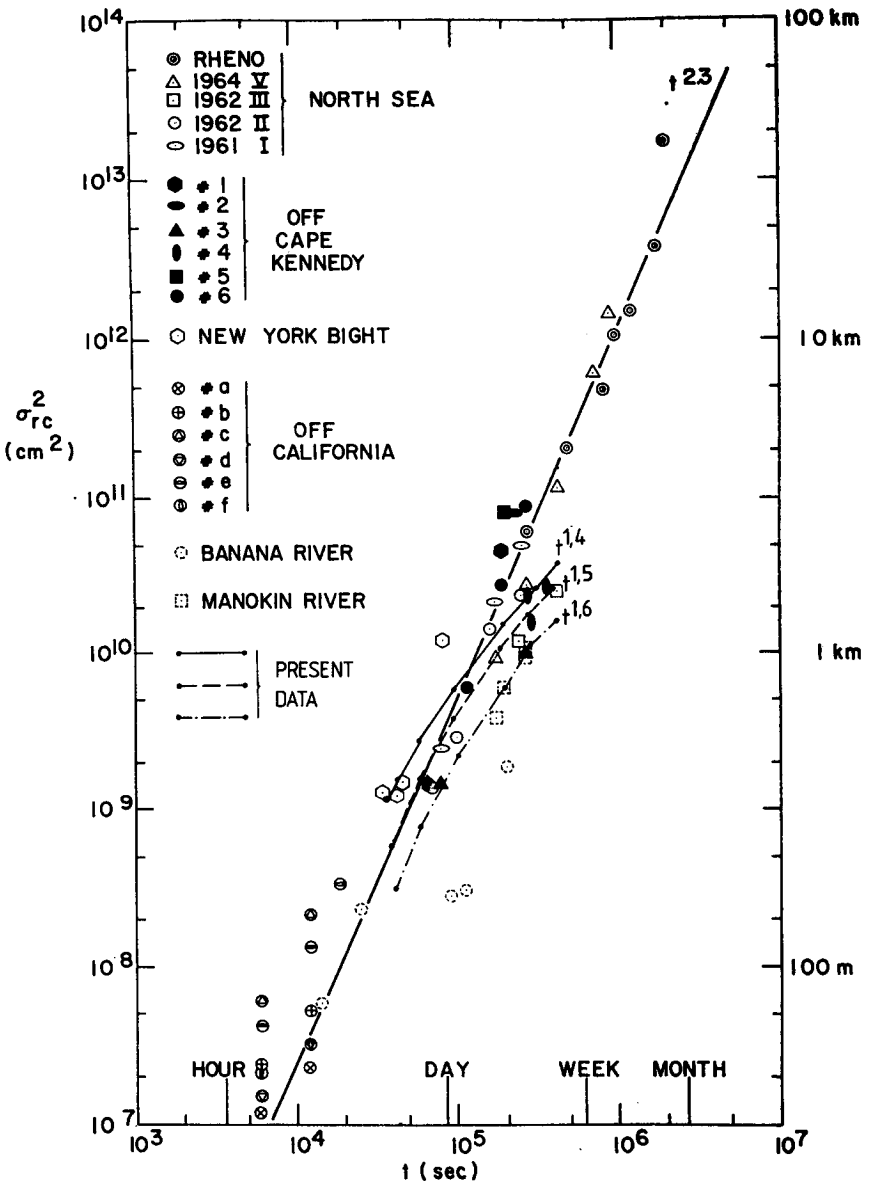

FIG. 7. As in Fig. 6 but for $C_r = 0.3$.

5. Conclusions

A Markov chain simulation of fluid particle velocities along a given velocity gradient can be used to determine the dispersion of some tracer in a turbulent boundary layer. The velocity field and turbulence intensity change markedly across a boundary layer flow, as do the length and time scales of turbulence. Such inhomogeneities will influence the movement and spread of any marked fluid element introduced into the flow. The present model combines stochastic velocity fluctuations in the vertical with a horizontal turbulent shear flow.

A one-dimensional model including an advanced turbulence model yields both the horizontal velocity field and some statistical properties of the flow. This information is then used in a Markov chain that determines the vertical velocity fluctuations. The Markov chain is based on the deterministic Langevin's equation. This equation is modified to include the effect of a mean pressure gradient due to the gradient in vertical velocity variance caused by the boundary conditions. However, the turbulence model is formulated within an Eulerian frame of reference, while Langevin's equation—and hence the Markov chain—is based on the Lagrangian counterpart. In particular, the time scale

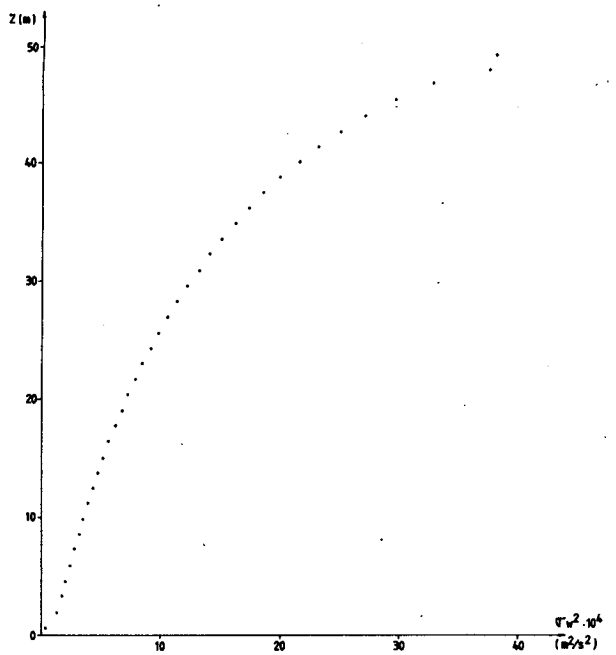

FIG. 8. The instantaneous distribution of the Lagrangian velocity variance σ_w^2 vs height.

τ_E as well as the variance σ_{wE}^2 cannot be rigorously related to their Lagrangian counterparts, though empirical relations are assumed in both cases.

The properties of the $k - \epsilon$ model are well documented in literature, but the use of Langevin's equation is based on some hypothesis not rigorously verified in an oceanographic context. Hence, in order to gain some confidence in this model, a plane Poiseuille flow was considered. The predicted dispersion agreed very well with independent theoretical estimates presented in literature. Hence this result encourages an attempt to model dispersion in a turbulent Ekman layer. The $k - \epsilon$ model has already been applied to this boundary layer with good results.

Characteristic properties, based on the behavior of clusters of particles, confirm with corresponding results from tracer studies carried out in the oceanic surface layer. On short time scales the cluster growth is qualitatively in accordance with theoretical predictions. However, on larger time scales the evolution of the cluster was markedly slower than its counterparts in the field experiments. This is partly due to the choice of forcing, a unidirectional steady wind. Hence, variations of the calculated flow field on inertial length and time scales will govern this spread. This is evident in the evolution of K_x (see Fig. 10) where K_x reaches its asymptotic value after roughly 1–2 inertial periods. In the oceans, eddies on larger scales (mesoscales) will also influence the dispersion process. Hence, the chosen forcing is rather unrealistic in a geophysical context, especially on time scales of several days.

As a conclusion, the model seems to predict the hor-

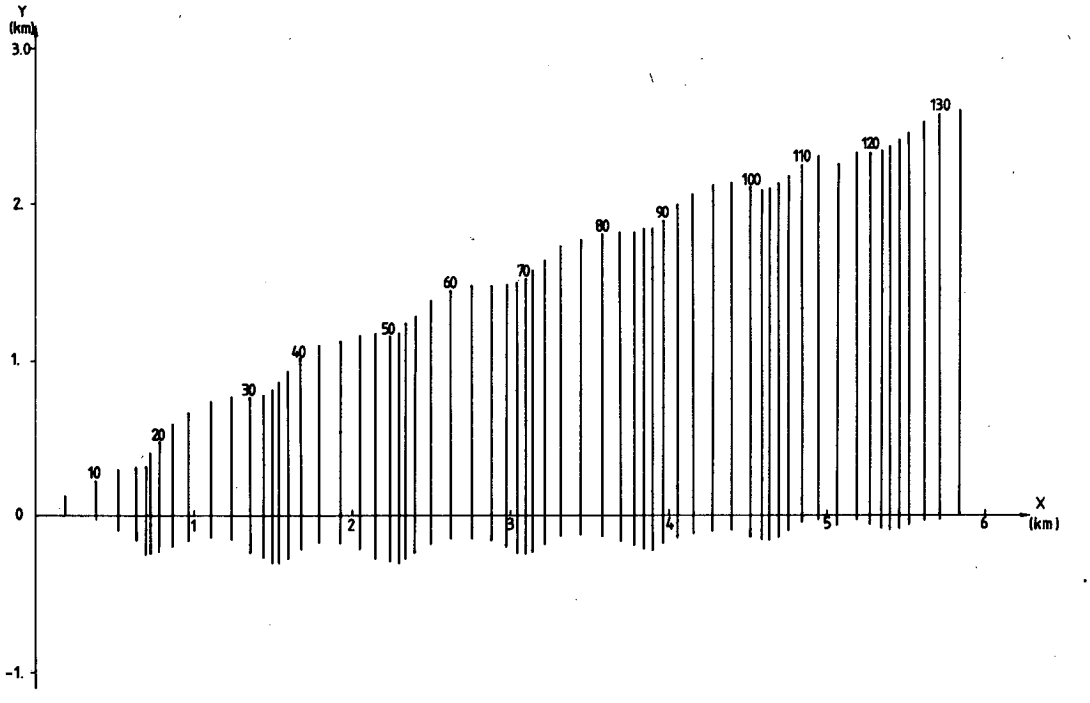

FIG. 9. The evolution of the cluster with time is illustrated by the displacement of the center of mass and its standard deviation σ_y. The time is indicated at every 10 hours. (The cluster was released at 6 hours).

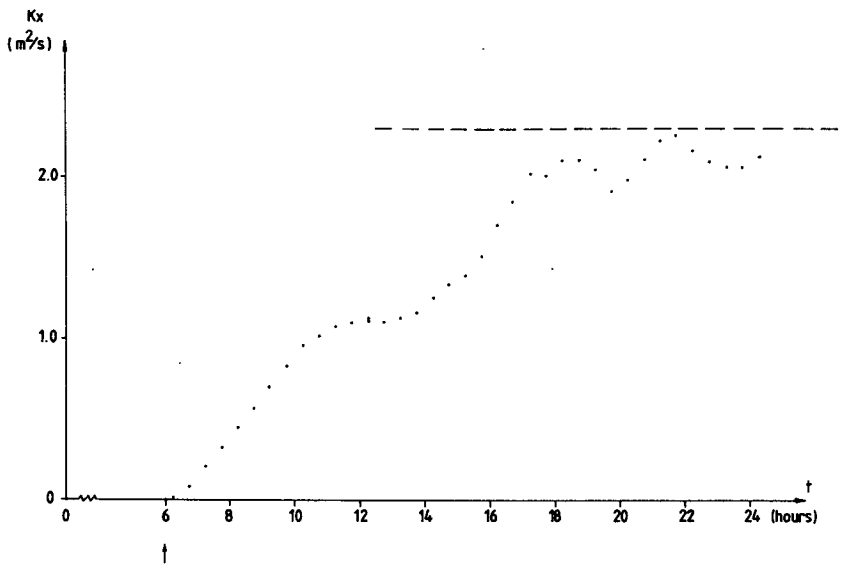

FIG. 10. The initial evolution of the apparent diffusivity K_x vs time. The dashed line represents the approximative steady-state value.

izontal dispersion rather well on time scales of a couple of days, despite the fact that it is based on only vertical mixing and vertical shear of a horizontal flow, the latter governed by Ekman layer dynamics. The predictions are rather unsensitive to variations in the empirical coefficients C_τ and C_σ. The model of Legg and Raupach (1982) is, however, based on a fixed time-step. In the present case with a turbulent Ekman layer, the variations over depth of Taylor microscale and Lagrangian integral time scale are such that the inequality (2.7) cannot be satisfied over the entire layer.

One consequence of this is that one obtains solutions that are to some degree time-step dependent. Though the resulting errors in the present case seem insignificant, it leaves scope for future improvements of the model. (Note that Thomson, 1984, has already pointed out that the validity of this dispersion model is limited to only weakly inhomogeneous turbulence.) Further, in order to improve the validity of the model on larger time scales, mesoscale processes must be included in some way, something which is beyond the scope of this work.

Acknowledgments. The authors wish to thank Mrs. V. Kuylenstierna for valuable help with the preparation of the manuscript.

REFERENCES

Arnold, L., 1974: *Stochastic Differential Equations: Theory and Applications.* Wiley-Interscience, 228 pp.

Batchelor, G. K., 1949: Diffusion in a field of homogeneous turbulence. I. Eulerian analysis. *Aust. J. Sci. Res.*, **A2**, 437–450.

Chandrasekhar, S., 1943: Stochastic problems in physics and astronomy. *Rev. Mod. Phys.*, **15**, 1–89.

Csanady, G. T., 1973: *Turbulent Diffusion in the Environment.* D. Reidel, 248 pp.

Dillon, T. M., and T. M. Powell, 1976: Low-frequency turbulence spectra in the mixed layer of Lake Tahoe, California–Nevada. *J. Geophys. Res.*, **81**, 6421–6427.

Elder, I. W., 1959: The dispersion of marked fluid in turbulent shear flow. *J. Fluid Mech.*, **5**, 544–560.

Hall, C. D., 1975: The simulation of particle motion in the atmosphere by a numerical random-walk model. *Quart. J. Roy. Meteor. Soc.*, **101**, 235–244.

Hanna, S. R., 1982: Applications in air pollution modelling. *Atmospheric Turbulence and Air Pollution Modelling,* F. T. M. Nieuwstadt and H. van Dop, Eds., D. Reidel, 358 pp.

Hay, J. S., and F. Pasquill, 1959: Diffusion from a continuous source in relation to the spectrum and scale of turbulence. *Advances in Geophysics,* Vol. 6, Academic Press, 345–365 pp.

Hinze, J. O., 1975: *Turbulence.* 2nd ed., McGraw-Hill, 586 pp.

Hussain, A. K. M. F., and W. C. Reynolds, 1975: Measurements in fully developed turbulent channel flow. *J. Fluids Eng.*, Dec., 568–578.

Krasnoff, E., and R. L. Peskin, 1971: The Langevin model for turbulent diffusion. *Geophys. Fluid Dyn.*, **2**, 123–146.

Lam, D. C. L., C. R. Murthy and R. B. Simpson, 1984: *Effluent Transport and Diffusion Models for the Coastal Zone.* Springer-Verlag, 168 pp.

Launder, B. E., G. J. Reece and W. Rodi, 1975: Progress in the development of a Reynolds-stress turbulence closure. *J. Fluid Mech.*, **68**, 537–566.

Legg, B. J., 1983: Turbulent diffusion from an elevated line source: Markov chain simulations of concentration and flux profiles. *Quart. J. Roy. Meteor. Soc.*, **109**, 645–660.

——, and M. R. Raupach, 1982: Markov chain simulation of particle dispersion in inhomogeneous flows: The mean drift velocity induced by a gradient in Eulerian velocity variance. *Bound. Layer Meteor.*, **24**, 3–13.

Madsen, O. S., 1977: A realistic model of the wind-induced Ekman boundary layer. *J. Phys. Oceanogr.*, **7**, 248–255.

Mollo-Christen, E., and S. Worthem, 1985: Oceanic transports by wave-induced fluxes. *Ocean Modelling,* **61**, 13–17.

Obukhov, A. M., 1959: Description of turbulence in terms of La-

grangian variables. *Advances in Geophysics,* Vol. 6, Academic Press, 113–116.

Okubo, A., 1971: Oceanic diffusion diagrams. *Deep-Sea Res.,* **18,** 789–802.

Pasquill, F., 1974: *Atmospheric Diffusion.* 2nd ed., Wiley and Sons, 297 pp.

——, and F. B. Smith, 1983: *Atmospheric Diffusion.* 3rd ed., Wiley and Sons, 437 pp.

Reid, J. D., 1979: Markov chain simulation of vertical dispersion in the neutral surface layer for surface and elevated releases. *Bound. Layer Meteor.,* **16,** 3–22.

Rodi, W., 1980: Turbulence models and their applications in hydraulics. *Int. Assoc. Hydrol. Res.,* Delft, 1–104.

Schott, F., and D. Quadfasel, 1979: Lagrangian and Eulerian measurements of horizontal mixing in the Baltic. *Tellus,* **31,** 138–144.

Shir, C. C., 1973: A preliminary numerical study of atmospheric turbulent flows in the idealized planetary boundary layer. *J. Atmos. Sci.,* **30,** 1327–1339.

Smith, F. B., 1968: Conditioned particle motion in a homogeneous turbulent field. *Atmos. Environ.,* **2,** 491–508.

Svensson, U., 1978: A mathematical model of the seasonal thermocline. Ph.D. dissertation, Rep. 1002, Dep. Water Resour., University of Lund, Sweden, 187 pp.

——, 1979: The structure of the turbulent Ekman layer. *Tellus,* **31,** 340–350.

Taylor, G. I., 1921: Diffusion by continuous movements. *Proc. Lond. Math. Soc.,* Ser. 2, **20,** 196–212.

——, 1953: Dispersion of soluble matter in solvent flowing slowly through a tube. *Proc. Roy. Soc.,* **A219**(1137), 186–203.

——, 1954: The dispersion of matter in turbulent flow through a pipe. *Proc. Roy. Soc.,* **A223**(1155), 446–468.

Tennekes, H., and J. L. Lumley, 1972: *A First Course in Turbulence.* MIT Press, 300 pp.

Thompson, D. J., 1984; Random walk modelling of diffusion in inhomogeneous turbulence. *Quart. J. Roy. Meteor. Soc.,* **110,** 1107–1120.

Uhlenbeck, G. E., and L. S. Ornstein, 1930: On a theory of Brownian motion. *Phys. Rev.,* **33,** 823–841.

Wax, N., 1954: *Selected Papers on Noise and Stochastic Processes.* Dover, 337 pp.

Wilson, J. D., G. W. Thurtell and G. E. Kidd, 1981: Numerical simulation of particle trajectories in inhomogeneous turbulence. II: Systems with variable turbulent velocity scale. *Bound.-Layer Meteor.,* **21,** 423–441.

——, B. J. Legg and D. J. Thomson, 1983: Calculations of particle trajectories in the presence of a gradient in turbulent-velocity variance. *Bound.-Layer Meteor.,* **27,** 163–169.

Young, W. R., P. B. Rhines and C. J. R. Garrett, 1982: Shear-flow dispersion, internal waves and horizontal mixing in the ocean. *J. Phys. Oceanogr.,* **12,** 515–527.

Zeman, O., and H. Tennekes, 1975: A self-contained model for the pressure terms in the turbulent stress equations of the neutral atmospheric boundary layer. *J. Atmos. Sci.,* **32,** 1808–1813.

Zilitinkevich, S. S., D. L. Laikhtman and A. S. Monin, 1967: Dynamics of the atmospheric boundary layer. *Atmos. Oceanic Phys.,* **3,** 297–333.